Hindawi
Journal of Engineering
Volume 2022, Article ID 2273819, 11 pages
https://doi.org/10.1155/2022/2273819

Research Article

Performance of MOSFET Driven via a Bootstrap Capacitor for Dynamic Load Continuity Enhancement

Hamdy Abd El-Halim, El Sayed Soliman, and Amr Refky

Department of Electrical Engineering, Faculty of Engineering, Al-Azhar University, Cairo, Egypt

Correspondence should be addressed to Amr Refky; amrrefky@azhar.edu.eg

Received 21 February 2022; Revised 4 April 2022; Accepted 3 May 2022; Published 19 May 2022

Academic Editor: Yuh-Shyan Hwang

In this paper, the operation and a complete design of the bootstrap circuit elements when firing a high-side MOSFET feeding an inductive load are introduced. The operation for both low-side and high-side cases are discussed with complete design and analysis of the bootstrap circuit elements. The effect of the bootstrap capacitor (BSC), diode, and resistance on the MOSFET switch for inductive loads at different frequencies and duty cycles including regular and SPWM are briefly analyzed. The current discontinuity is associated with higher losses, discontinued power output operation, and derated performance. The precise good design of the bootstrap circuit elements enables to improve the load current continuity in a specified frequency range of operation preventing the demerits of discontinuous operation. The effect of high-side implementation on extra harmonic content on the load is discussed including THD measurement of both applied voltages and currents.

1. Introduction

The MOSFET (Metal Oxide Semiconductor Field Effect Transistor) switch is a voltage-controlled electronic device preferred for switching application due to its high switching frequency in addition to its lower losses during conduction and switching cases [1–4]. When the driving circuit of the electronic switches is not properly designed, the switch block status occurs. A distinguished difference for switching the MOSFET or IGBT for low- and high-side cases is clear due to the driving signal reference voltage [1,5]. In the low-side case, where the load is usually above the switch, the gate-to-source voltage is referred to the zero-source value and the switching has no problems.

The MOSFET will directly switch on for gate voltages greater than the source value by a specified drop according to the switch input impedance and capacitance in addition to its other characteristics [4–6]. In case of high side, where the load is below the switch, the gate-to-source voltage depends on the load voltage, which is variable. Any partial turns of the MOSFET switch due to low values of the gate-to-source voltage will increase the conduction drain-to-source resistance resulting in higher losses with extra heat and may damage the MOSFET [6–8]. Operation of the high-side switch must fulfill an appropriate level shift of the gate voltage above the load value to ensure good switching of the MOSFET. Different techniques are used to fulfill this difference, the most common being the bootstrap method. The implementation of N-channel MOSFET driving instead of P-Channel driving is preferable to avoid positive terminal reference and to introduce high efficiency [1, 5, 7, 9]. One advantage is that the extra circuitry added will affect the overall efficiency of the driving system. Different driving ICs are used for electronic switching allowing the use of the bootstrap elements with complete designed values to verify the appropriate switching modes. It is important when high-side driving is implemented to reduce the parasitic effect. So, precautions such as thick and direct tracks and avoiding lead inductance and interconnected links are influential [9–11].

2. Bootstrap Circuit Operation

For power conversion circuits such as single-phase and three-phase full-bridge converters, a half-bridge topology is

considered as a core component. As the high-side switch has a floating ground, two independent power supplies are usually necessary to control the gates of both high-side and low-side power switches. This is a significant issue when it comes to miniaturizing power converter circuits. The techniques of bootstrapping and charge pumping have been proposed as potential solutions to this issue [1, 3]. The main bootstrap circuit elements are a bootstrap capacitor, a fast-switching diode, a limiting resistor, and a bypass larger capacitor. The bootstrap circuit elements are designed before implementation according to the proposed process and application. During the off interval, the capacitor must be appropriately charged to a specified voltage above the load point voltage. It is reliable to charge the bootstrap capacitor to an initial value for a certain time before operation [2, 8, 9]. At the first glance, the bootstrap circuitry appears as a simple, low-cost mechanism consisting of a BSC, a diode, and a resistor, but potential design of the circuit elements is associated. The bootstrap capacitor value depends on the switching frequency of the MOSFET [12–15]. Charging is usually achieved via a fast-switching diode (Schottky diode) through a bootstrap-limiting resistance. The discharge of the capacitor is achieved via a predesigned resistor to be ready for the next on interval. Practically, the BSC must be charged and discharged within a certain level of voltages, not allowing the capacitor voltage to reach zero any way. The capacitor is charged from a low-voltage source with small power consumed to drive the gate. The range of the operation frequency rather than the implemented duty cycle must be taken into account [3, 15, 16].

2.1. Drawback of Bootstrap Circuitry. The bootstrap circuit is simple and of low cost. The BSC is limited to the operating frequency and duty cycle. The main difficulty for low- and high-side switches at the same arm is the flow of the load current suddenly in the low-side freewheeling diode as a result of the negative voltage appearing at the source. Another problem caused by the negative voltage transient is the possibility to develop an overvoltage condition across the bootstrap capacitor [9, 17].

2.2. Analysis and Design of the Bootstrap Circuit

2.2.1. The Bootstrap Capacitor. The BSC provides a low impedance path for sufficient charges to charge the high-side switch. A practical value of the BSC must at least exceed ten times the gate capacitance of the MOSFET to avoid malfunctioning due to temperature and load transients. The BSC minimum value must be included to avoid permanent turning-off of the high-side MOSFET; on the other hand, greater values of the BSC lead to smaller capacitor voltage ripples in addition to longer reverse recovery time which leads to malfunctioning of the driving circuit. The design of the BSC includes three main parts; the drive circuit, the MOSFET switch parameters, the BSD ratings, and the BSC specifications. The bootstrap capacitor is charged only when the low-side power switch is turned on and discharged when a high-side switch is turned on [17–19]. To maintain gate-source voltage within an acceptable minimum value, the capacitor voltage drop must be

$$\Delta V_{bs} = V_{D\,D} - V_{F\,D} - V_{GS_{\min}} - V_{SW}. \tag{1}$$

The voltage drop across the MOSFET depends on its conduction drain-to-source resistance and the load current.

$$V_{SW} = R_{DS} I_D. \tag{2}$$

The total leakage current is determined from

$$I_{\delta t} = I_{\delta_{BSC}} + I_{\delta_{GS}} + I_{\delta_Q} + I_{\delta_{off}} + I_{\delta_D}. \tag{3}$$

The bootstrap capacitor leakage current is usually omitted for nonelectrolytic capacitors, which imposes us to usually use a nonelectrolytic BSC. The total charge which must be supplied from the BSC to be injected to the gate to achieve MOSFET switching is

$$Q_t = Q_g + Q_{ls} + t_{on} I_{\delta t}. \tag{4}$$

The minimum value of the BSC is given from

$$C = \frac{Q_t}{\Delta V_{bs}}. \tag{5}$$

The charge required by the internal level shifter according to the rated applied voltage is in the range (3–20 nC) for rated voltages from 500 to 1200 V. It is recommended to use the BSC of value about 2–3 times the minimum designed value to avoid overcharging. A decoupling capacitor may be used in addition to mitigate low-frequency drains on the supply [17, 19, 20]. The applicable values of the capacitor for a duty cycle of 50% at different frequencies and different duties at a frequency of 50 Hz are shown in Figure 1

2.2.2. The Bootstrap Diode and Resistor. When the high-side device is turned on, the bootstrap diode must be able to block the full-power rail voltage. To reduce the amount of charge fed back from the bootstrap capacitor into the *Vcc* supply, it must be a fast recovery diode and a high-temperature reverse leakage current would be significant if the capacitor had to retain charge for lengthy periods of time [7, 9]. A series-limiting resistance bootstrap (BSR) is always considered to avoid inrush currents through the BSD, especially at startup to minimize the noise spikes. The BSR in series with the BSC will provide a retardation of the voltage rate in addition to the charging time constant of the BSC. Optimum design is required to avoid any damage of the circuit components rather than maintaining a reliable time constant of the BSC circuit. The chosen BSR must withstand the high power dissipation during charging of the BSC. The minimum charging time of the BSC must be verified against the time constant. The voltage drop across the BSC and its value affect directly the power dissipation in the BSR since a higher voltage drop will not allow a sufficient charging time [16, 17, 20]. Moreover, this work has been used with a BSD of 220V and a resistor of 1 Ω (typical values of BSR are 3 to 10 Ohms).

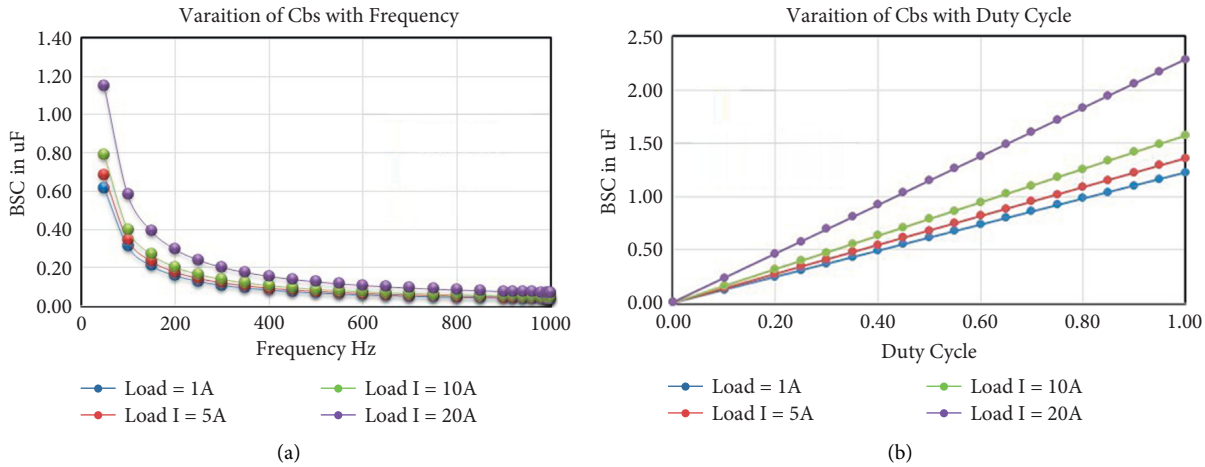

Figure 1: BSC variation with frequency and duty cycle at different loads.

2.2.3. The Bootstrap Circuit Switching Analysis. The most popular model circuit of the bootstrap technique of driving a MOSFET is shown in Figure 2. The BSC charges when *SW1* and *SW2* are on, and the discharge occurs when *SW1* and *SW2* are off through the paths shown in Figure 3.

Indeed, the system scenarios can be presented as follows: the on state during which the BSC will be partially charged and the off state during which the discharge process is achieved. The BSC is charged every time the low-side driver is switched on, and the output pin is below the supply voltage *VDD* of the gate driver. The BSC is discharged only when the high-side switch is turned on. This bootstrap capacitor is the gate-to-source driving supply voltage for the high circuit section. The first parameter to be considered is the maximum voltage drop that we have to guarantee when the high-side switch is in on state. The maximum allowable voltage drop (VBOOT) depends on the minimum gate drive voltage (for the high-side switch) to maintain [19, 20].

2.2.4. System Modeling Circuit. The proposed high-side driving model using MATLAB is shown in Figure 4. The previous circuit is represented considering different PWM sources, and the MOSFET switch is used to drive an inductive load. The measure and analysis of all voltage and current waves for both the BSC circuit and the inductive load are investigated. The power dissipated in the load part rather than that drawn by elements of the bootstrap circuit elements was measured. The system performance is investigated under different PWM signals with multivalued bootstrap capacitors and different frequencies. The bootstrap capacitor will have maximum and minimum values to ensure switching of the MOSFET at high-side operation. The capacitor peak-to-peak voltage, current, load voltage, and load current are investigated for different modes of operation. For an inductive load with $R = 1\Omega$ and $L = 10mH$, the system performance for a BSC of 10μF with a PWM at 50Hz with a duty cycle of 0.5 is shown in Figure 5. The performance with different values of BSC is shown in Figures 6, 7, 8, and 9. The low frequency (from 50 to 1000 Hz) is adopted to visualize the effect of the BSC on the load current

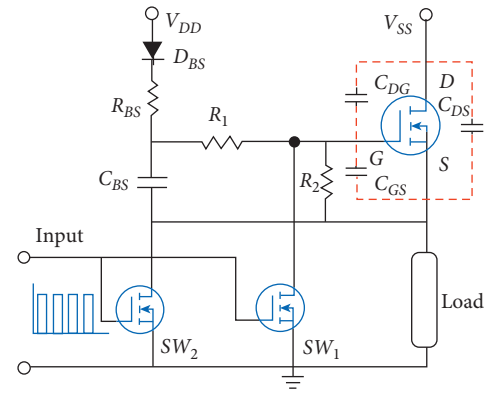

Figure 2: Bootstrap circuit for high-side switching.

continuity since high frequency is usually associated with a continuous current mode.

The system performance at different frequencies is now discussed. The simulated model demonstrates the system response for different operation modes.

2.3. Continuous Current Mode. In this mode, with different data and parameters given in Table 1, the system response is shown in Figure 5. The BSC voltage and load performance parameters are discussed in addition to the harmonic analysis of the load current.

2.4. Discontinuous Current Mode. A discontinuous current mode is associated with zero values of the load current. All load parameters in addition to the drive circuit operation frequency and on time are effective in the load current continuity. The new mode is now analyzed only with a change of load inductance to be 20mH. The system response is shown in Figure 6.

However, the discontinuous current mode is not recommended in most drives, and it has been discussed for estimating the suitable bootstrap circuit parameters by which a proposed continuous operation can be achieved in the next paragraph.

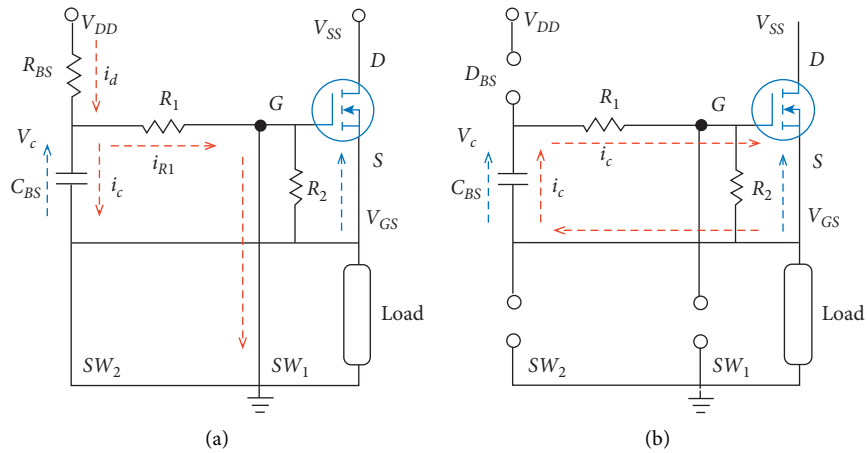

Figure 3: The charging and discharging modes of the bootstrap capacitor.

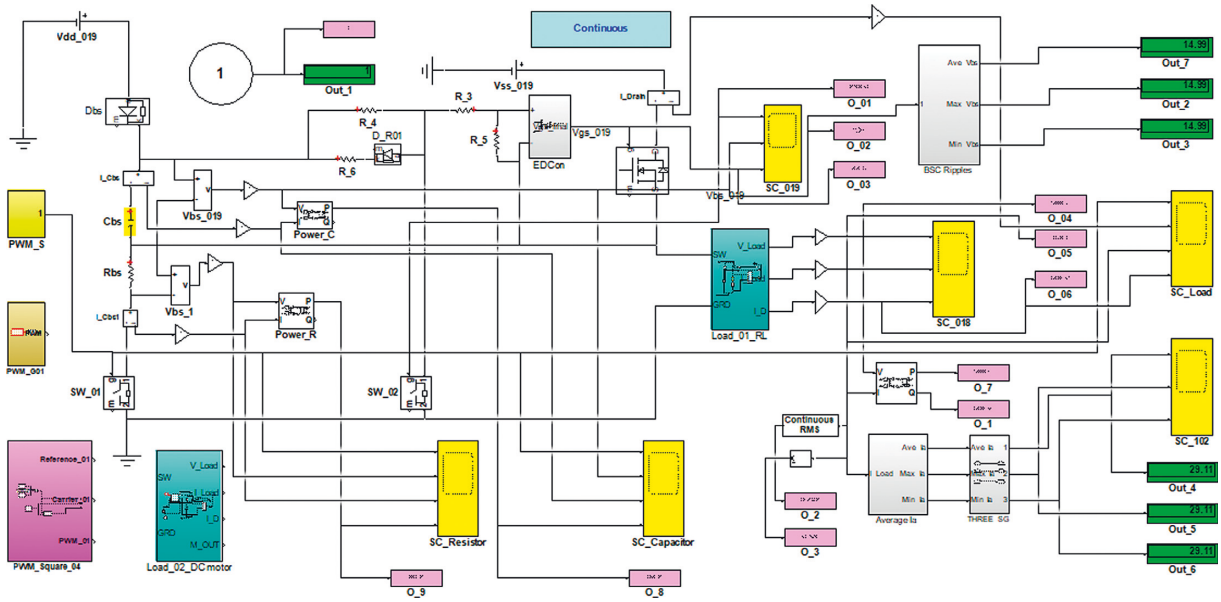

Figure 4: The bootstrap high-side MOSFET switching.

It is obvious from the simulated results that the BSC value voltage ripples change with frequency and load current. Hence, the frequency range of operation is determined for good calculation of the BSC value. Lowering the charging time constant cannot sustain a desirable range of the peak-to-peak capacitor voltage. Usually, the BSD offers a good time constant, especially when it is a fast switching diode.

3. Bootstrap Enhancement System

The operation of inductive loads from the high-side MOSFET involves different modes of the current passing through the load. The continuous current mode is associated with low harmonic content rather than optimized performance of the inductive load and effective performance of dynamic loads such as DC motors. The continuous and discontinuous modes are shown in Figure 7. Due to a direct relation between the on time and the average current flow through the MOSFET, the value of the BSC is precisely tuned to achieve continuous current operation, leading to advanced performance of the inductive load. When a DC chopper is feeding an inductive load with a back emf, the current continuity is affected by the load parameters in addition to the operation characters of the DC chopper such as the duty cycle and the switching frequency.

The continuous and discontinuous current modes are shown in the expression of the minimum and maximum currents.

$$I_1 = \frac{(V_s/R)\{\exp\{(T/\tau)\} - 1\}}{\{\exp\{(T/\tau)\} - 1\} - (E/R)}, \tag{6}$$

$$I_2 = \frac{(V_s/R)\{1 - \exp\{(-t_{on}/\tau)\}\}}{\{1 - \exp\{(-T/\tau)\}\} - (E/R)}. \tag{7}$$

With the time constant $\tau = L/R$, the approximate value of the average current is $I_{av} = 0.5(I_1 + I_2)$ and is given by

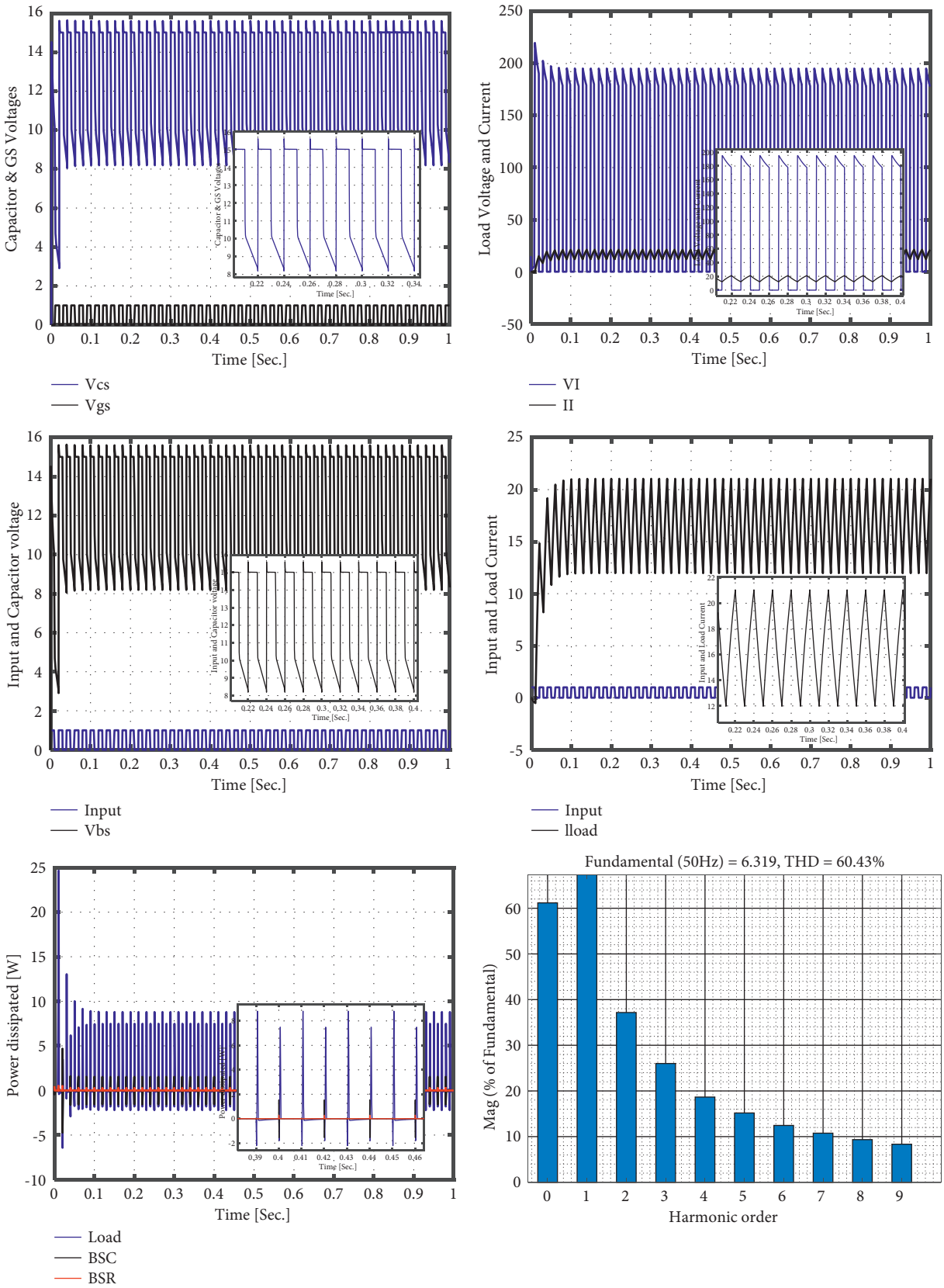

Figure 5: The system performance for a continuous current mode.

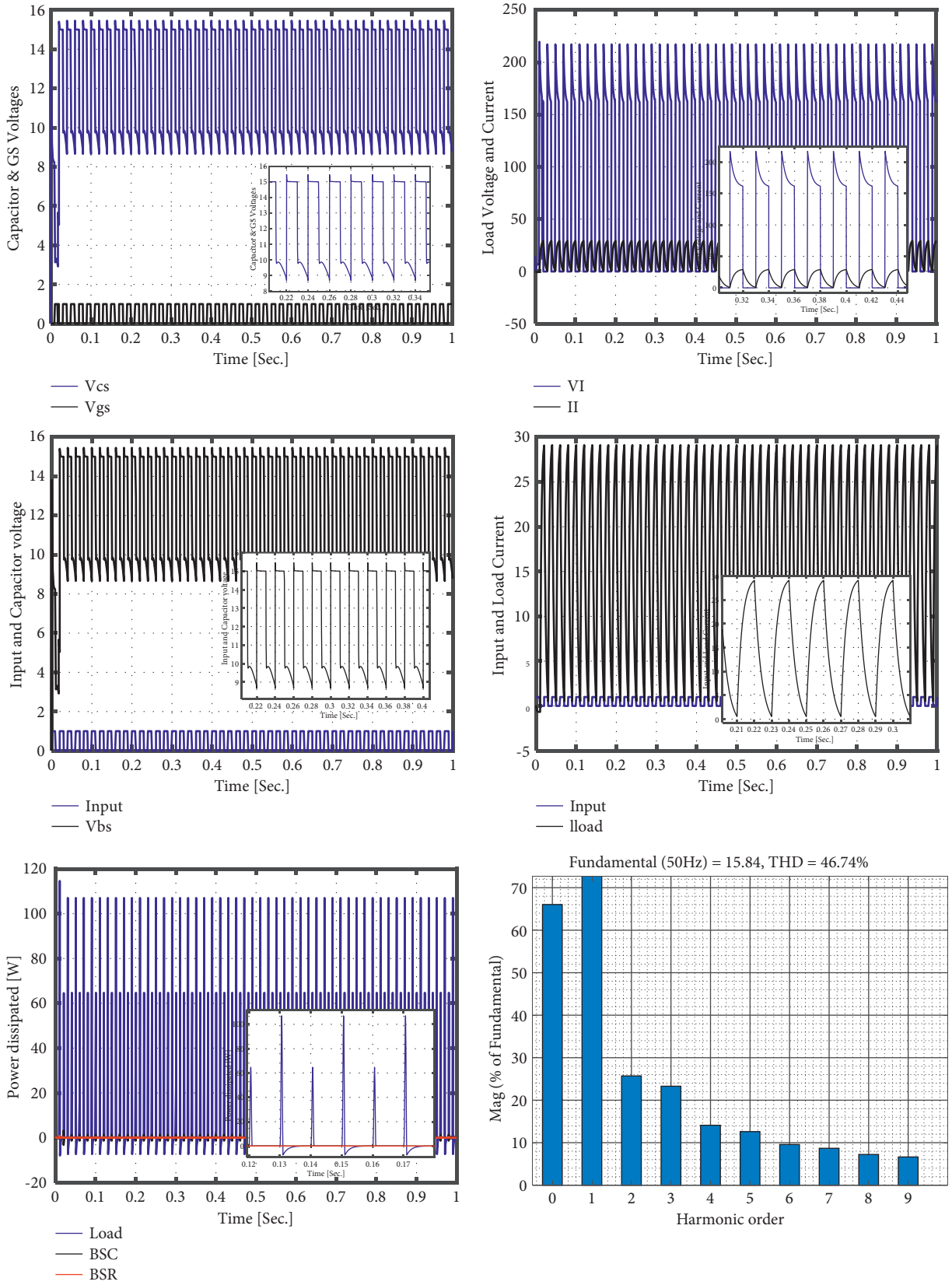

Figure 6: The system performance for a discontinuous current mode.

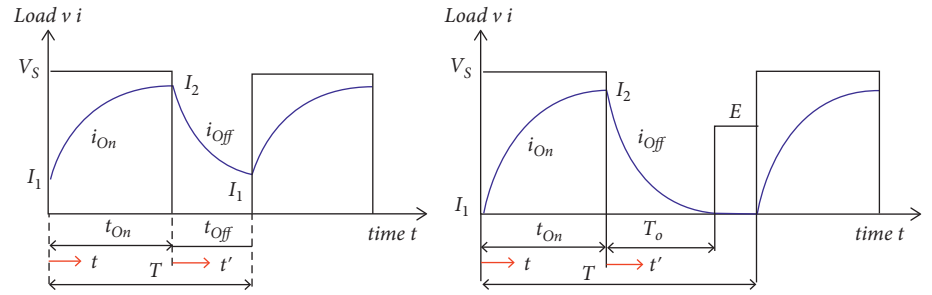

Figure 7: Continuous and discontinuous load current modes.

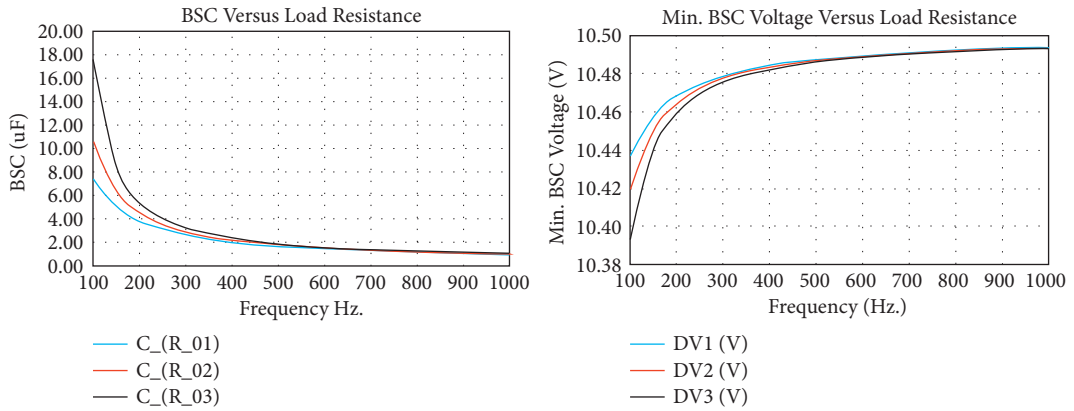

Figure 8: Variation of the BSC and minimum voltage with frequency at different load resistances.

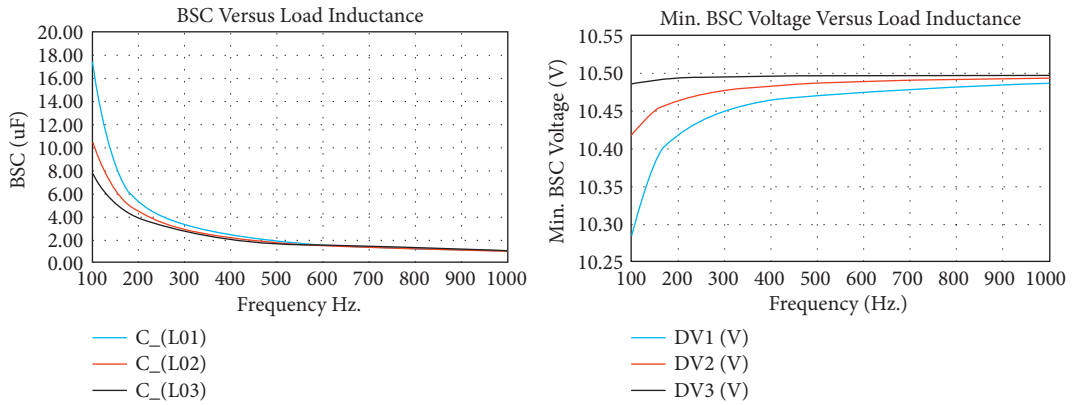

Figure 9: Variation of the BSC and minimum voltage with frequency at different load inductances.

Table 1: Continuous current mode parameters.

Drive circuit	BS parameters	Load parameters
PWM	$C_{BS} = 10\mu F$	$V_s = 220V$
$50Hz$	$R_{BS} = 0.1\Omega$	$R_a = 5\Omega$
$D = 0.5$	$V_{D\,D} = 15V$	$L_a = 100mH$
	$R_{DB\,S} = 1.2\Omega$	$E_b = 10V$

$$I_{av} = \frac{(V_{av} - E)}{R_a = (DV_s - E)/R_a}, \tag{8}$$

The transfer point between continuous and discontinuous modes is the point at which the current reaches zero value at the end of the cycle. At this point, the BSC is calculated to ensure a current continuity. A conclusion is that the BSC minimum value must be verified in addition to that value which ensures current continuity. The transfer point is verified when reaching the total time of the cycle from

$$T = \tau \ln\left\{1 + \left(\frac{V_s}{E} - 1\right)\left\{1 - \exp\left\{\frac{-t_{on}R}{L}\right\}\right\}\right\}. \tag{9}$$

The minimum on time of the cycle to fulfill continuity is then

$$t_{on} = \tau \ln\left\{\frac{(V_s - E)}{(V_s - E) - E\{\exp(T/\tau) - 1\}}\right\}. \tag{10}$$

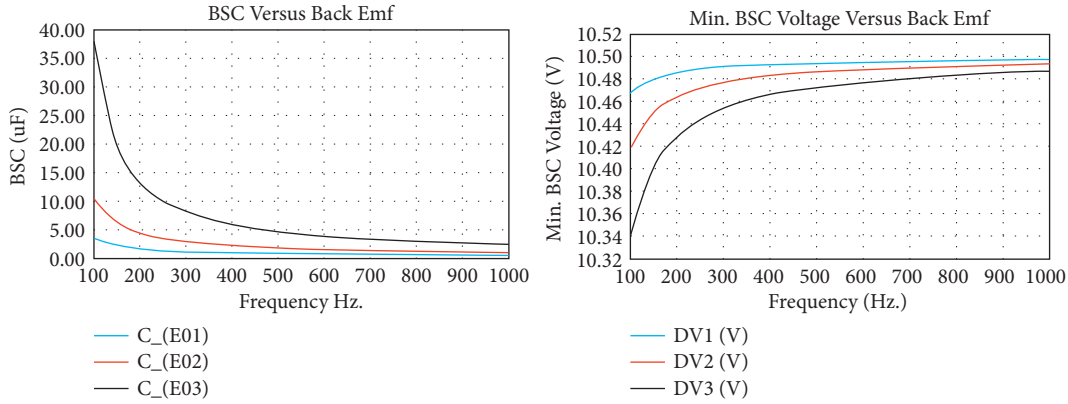

Figure 10: Variation of the BSC and minimum voltage with frequency at different back emfs.

This average current in this case with zero minimum value is given from

$$I_{av} = 0.5\left(\frac{V_s - E}{R}\right)\left\{1 - \exp\left\{\frac{-t_{on}}{\tau}\right\}\right\}. \quad (11)$$

The current continuity compensation is achieved by increasing the BSC value by the following value:

$$C = \frac{Q_g + Q_{ls} + t_{on}I_{\delta t}}{V_{DD} - V_{FD} - V_{GS\min} - R_{DS}I_{av}}. \quad (12)$$

Precisely determined values of the BSC to fulfill the current continuity are calculated in addition to the average current at different frequencies as the main effective parameter.

4. Different Load Compensations

4.1. Resistive Load. The increase of the load resistance usually lowers the time constant, leading the system to the discontinuity region. The variation of the BSC value and associated voltage according to the variation of the load resistance is shown in Figure 8. Increasing the load resistance requires a higher value of the BSC to fulfill continuous operation. It is convenient that for high frequencies, the BSC will be lower since the system naturally goes to the continuous current region.

4.2. Inductive Load. Normally, the highly inductive load results in a continuous current. The ally lowers the time constant, leading the system to the discontinuity region. The variation of the BSC according to the variation of the load inductance is shown in Figure 9.

4.3. Back emf. When the back emf increases, the system easily enters the discontinuity region. So, the value of the BSC required for compensation will increase. The variation of the BSC according to the variation of the back emf is shown in Figure 10.

It is clear from Figures 8–10 that the parameters forcing the load to the continuity mode of current are affected by the BSC value. The values calculated are the minimum values to ensure the current continuity. The major factor in this analysis is the on time during each cycle, which is directly adjusted from the load parameters to skip the transition point between continuity and discontinuity. It is obvious that the increase of the time constant or lowering the back emf directly drives the load to the continuity region.

5. Experimental Setup

The verification of the system is experimentally established by using an N-channel MOSFET switch (IRFP450) in a high-side mode of operation. The implemented system is fed from a controlled PWM generated from the Arduino kit with different frequencies and duty cycles. The circuit driver providing the bootstrapping technique in addition to both low-side and high-side driving is Integrated circuit IR2304. The complete PRB layout is shown in Figure 11. The experimental setup in addition to the capacitor charging and discharging maintaining a reliable peak-to-peak voltage value is shown in Figure 12.

The system results at different duty cycles and operating frequencies including different PWM signals are shown in Figures 13, 14 and 15

The system is verified experimentally by implementing the proposed hardware. A PWM signal is applied to the bootstrap circuit and drive a high-side MOSFET switch which drives an inductive load. The output from the drive circuit with different frequencies was discussed specially for low-frequency operation as shown in Figure 15. A declared operation of the BSC including charging and discharging periods keeping a specified capacitor ripple voltage is shown in Figure 12. The experimental work showed a reliable verification of the simulation results scoping on the effect of the BSC on current continuity.

In accordance with the previous analytical approach, the variation of the proposed high-side MOSFET switching circuit performance with the value of the BSC is verified experimentally. The load current for different duty cycles is measured at a low frequency (500 Hz) to fulfill the effect of the BSC on both the current status and switching mode of the MOSFET.

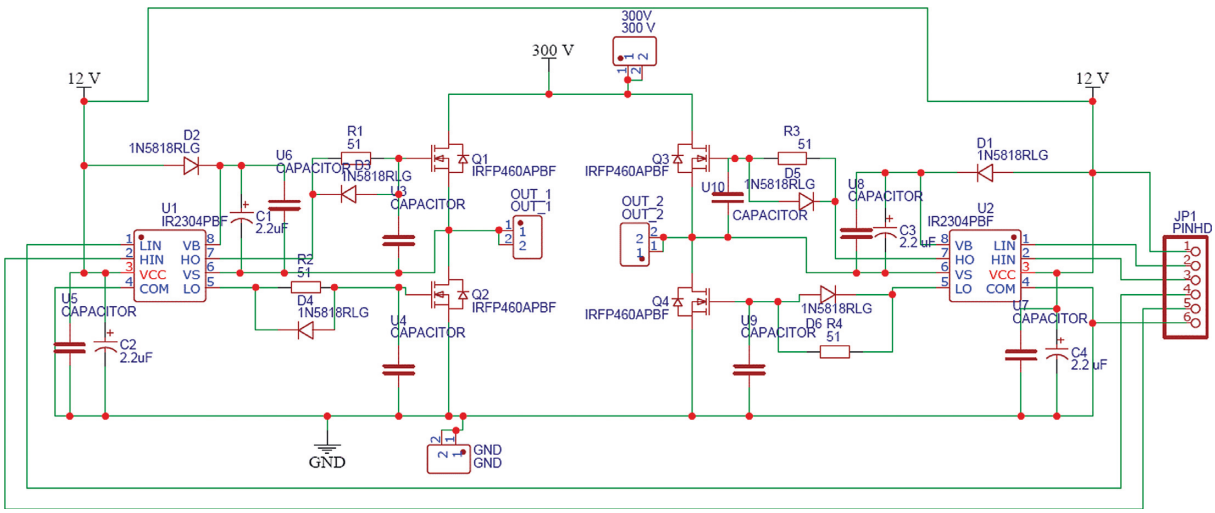

Figure 11: The H-bridge drive circuit fed from the PWM controlled Arduino signal.

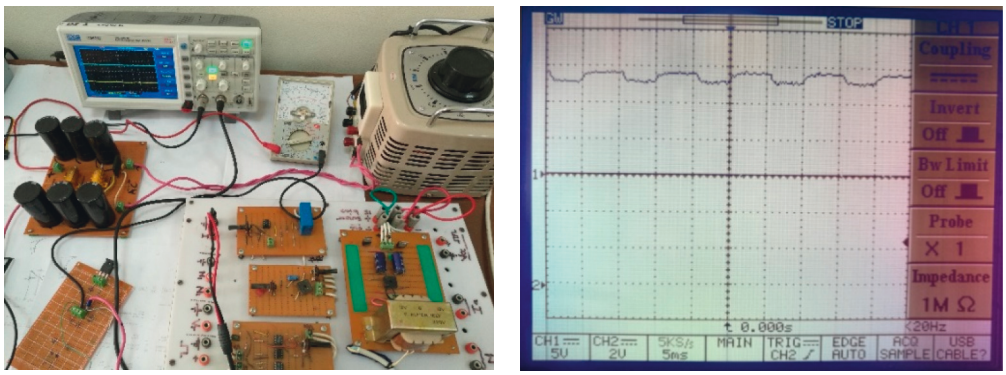

(a) (b)

Figure 12: The experimental setup and the capacitor voltage waves.

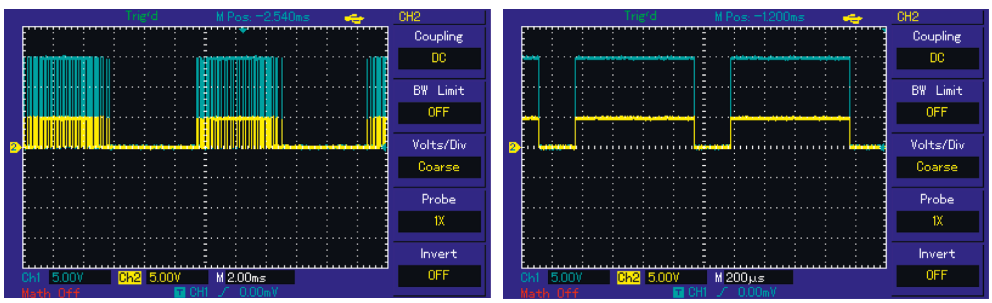

Figure 13: The generated waves and GS wave signals at different frequencies.

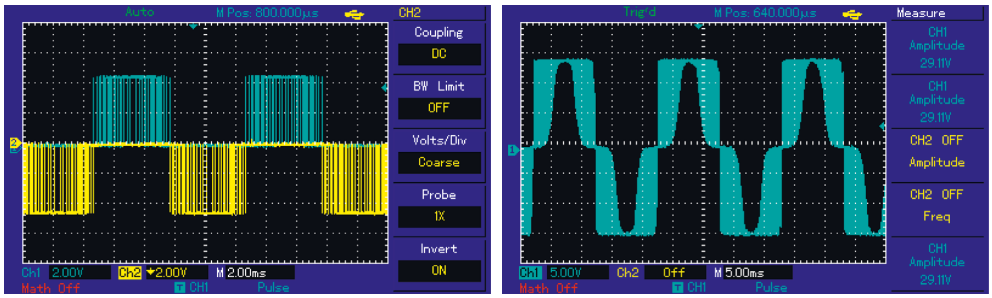

Figure 14: The generated waves from the Arduino IC.

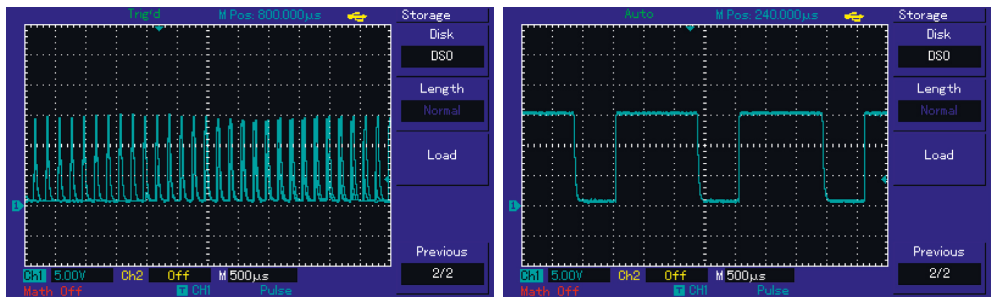

Figure 15: Charging and discharging of the BSC at different frequencies.

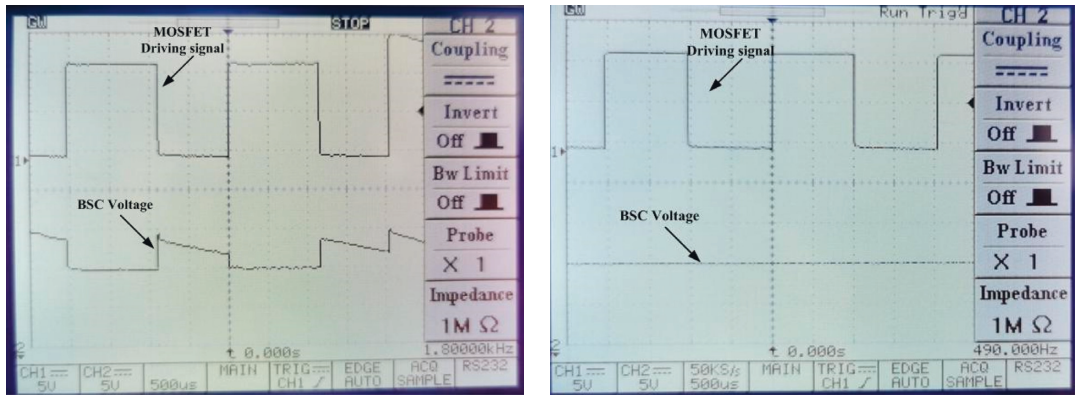

(a) (b)

Figure 16: Charging and discharging of the BSC (500 Hz, $D = 0.5$).

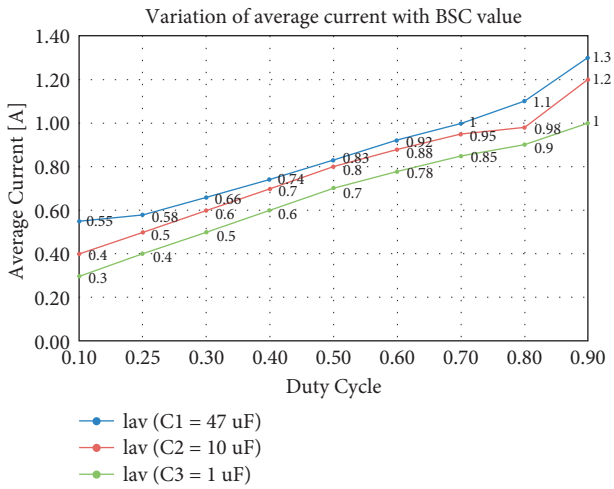

Figure 17: The average load current at different BSC values (500 Hz).

The considered load is slightly inductive since a higher inductive load leads highly to a continuous current mode. Exceeding the lower BSC value, the system operates with a current continuity status. For higher values of the BSC, the load approaches its continuity and the charge and discharge actions are low, producing a lower peak-to-peak capacitor voltage. The capacitor charging voltage at a minimum value of the BSC and larger values satisfying the reliable operation is shown in Figures 1616(a) and 16(b). The variation of the load current according to the BSC value at the minimum BSC value and larger values is also shown in Figure 17.

A reasonable relation proportion between the value of the average current and the BSC is shown from experimental records as shown in Figure 17.

6. Conclusions

The high-side switching using a bootstrap circuit technique was introduced. Steps of the complete design of the circuit elements including BSC, resistor, and diode were achieved with an experimental implementation by using a gate driver IC. The switching of the MOSFET at different PWM source voltages was introduced. The BSC must fulfill a specified range of maximum and minimum voltage during the charge and discharge intervals. The BSC is useful in high-side switch firing, but extra circuit arrangement is required with a correct design of the values according to the frequency and load requirements. The larger values of the BSC reduce the THD of load currents but are limited to values which reduce the peak-to-peak capacitor voltage. The BSC is a good solution to drive a dynamic load within the current continuity region to reduce harmonics and current fluctuations. A specified choice of the BSC improves the load current continuity as the switching periods of the MOSFET were directly related to the load continuity requirements. The direct relation between the on time and the average current flow through the MOSFET enables us to precisely choose the

value of the BSC to achieve continuous current operation, leading to an improved performance of the inductive load.

Abbreviations

BSC: Bootstrap capacitor
$V_{GS_{\min}}$: Minimum gate-to-source voltage
BS D: Bootstrap diode
$I_{\delta_{BSC}}$: Bootstrap capacitor leakage current
BSR: Bootstrap resistor
$I_{\delta_{GS}}$: Gate-to-source switch leakage current
ΔV_{bs}: The BSC voltage drop
I_{δ_Q}: Bootstrap circuit quiescent current
$V_{D\,D}$: Supply voltage of the gate driver
$I_{\delta_{off}}$: Offset supply leakage current
$V_{F\,D}$: Bootstrap diode forward voltage drop
I_{δ_D}: Bootstrap diode leakage current
V_{SW}: The voltage drop across the MOSFET
Q_g: The total gate charge
I_1: Minimum value of the load current
Q_{ls}: Charge by the internal level shifter
I_2: Maximum value of the load current
t_{on}: The on-duty of the cycle
V_S: Supply voltage of the load circuit
t_{off}: The off-duty of the cycle
τ: The load time constant
D: Duty cycle of the chopper drive circuit.

Data Availability

Data are available upon request via the corresponding author.

Conflicts of Interest

The authors declare that they have no conflicts of interest.

References

[1] Se-K. Chung and J.-G. Lim, "Design of bootstrap power supply for half-bridge circuits using snubber energy regeneration," *Journal of Power Electronics*, vol. 7, no. No. 4, 2007.

[2] M. J. Carra, Hernan Tacca, and J. Lipovetzky, "Performance evaluation of GaN and Si based driver circuits for a SiC MOSFET power switch," *International Journal of Power Electronics and Drive Systems*, vol. 12, no. 3, p. 1293, 2021.

[3] G. J. Wakileh, *Power System Harmonics*, , pp. 978–983, Springer-Verlag Berlin Heidelberg, 200I.

[4] R. Ali, I. Daut, S. Taib, N. S. Jamoshid, and A. R. A. Razak, "Design of high-side MOSFET driver using discrete components for 24V operation," vol. 2010, , pp. 132–136, PEOCO), 2010.

[5] M. H. Rashid, *Power Electronics, Circuits, Devices, and Applications*, Prentice-Hall, 3rd Edition, 2003.

[6] M. J. Mnati, A. H. Ali, D. V. Bozalakov, S. Al-yousif, and A. V. d. Bossche, "Design and implementation of a gate driver circuit for three-phase grid tide photovoltaic inverter application," *ICRERA*, vol. 2018, pp. 701–706, 2018.

[7] J. Zhu, W. Sun, Y. Zhang et al., "An integrated bootstrap diode emulator for 600-V high voltage gate drive IC with P-sub/P-epi technology," *IEEE Transactions on Power Electronics*, vol. 31, no. 1, pp. 518–523, 2016.

[8] H. Chen, L. He, H. Deng, Y. Yin, and F. Lin, "A high-performance bootstrap switch for low voltage switched-capacitor circuits," *IEEE International Symposium on Radio-Frequency Integration Technology*, vol. 2014, pp. 1–3, 2014.

[9] W. C. Chen, Y. W. Chou, M. W. Chien et al., "A dynamic bootstrap voltage technique for a high-efficiency buck converter in a universal serial bus power delivery device," *IEEE Transactions on Power Electronics*, vol. 31, no. 4, pp. 3002–3015, 2016.

[10] A. Soldati, E. Imamovic, and C. Concari, "Bidirectional bootstrapped gate driver for high-density SiC-based automotive DC/DC converters," *IEEE Journal of Emerging and Selected Topics in Power Electronics*, vol. 8, no. 1, pp. 475–485, 2020.

[11] T. Simonot, N. Rouger, and J. Crebier, "Design and characterization of an integrated CMOS gate driver for vertical power MOSFETs," *IEEE Energy Conversion Congress and Exposition*, vol. 2010, pp. 2206–2213, 2010.

[12] A. Seidel, M. Costa, J. Joos, and B. Wicht, "Bootstrap circuit with high-voltage charge storing for area efficient gate drivers in power management systems," *ESSCIRC*, vol. 2014, pp. 159–162, 2014.

[13] R. Stala, A. Mondzik, A. Penczek, Z. Waradzyn, and A. Skała, "All-bootstrap gate-driver supply system for a high-voltage-gain resonant DC-DC converter with seven switches," *Power Electronics and Drives*, vol. 5, no. 1, pp. 135–142, 2020.

[14] J. Garcia, S. Saeed, E. Gurpinar, A. Castellazzi, and P. Garcia, "Self-powering high frequency modulated SiC power MOSFET isolated gate driver," *IEEE Transactions on Industry Applications*, vol. 55, no. 4, pp. 3967–3977, 2019.

[15] B. Zhao, H. iong, R. Yang et al., "A Battery Powered Hybrid Dual-Path Step-Up DC-DC Converter with Output Powered Bootstrap Driver," *IEEE 14th International Conference on ASIC (ASICON)*, vol. 2021, pp. 1–4, 2021.

[16] G. Sharma, B. Joshi, and R. Orugnti, "A double bootstrap gate driving scheme for HERIC topology," *IEEE International Conference on Power Electronics, Drives and Energy Systems*, vol. 2018, pp. 1–6, 2018.

[17] N. Mitrovic, R. Enne, and H. Zimmermann, "A Bootstrap circuit for DC-DC converters with a wide input voltage range in HV-CMOS," *Electronics and Microelectronics (MIPRO)*, vol. 2016, pp. 62–65, 2016.

[18] M. Kong, W. Yan, and W. Li, "Design of a synchronous-rectified buck bootstrap MOSFET driver for voltage regulator module," *7th International Conference on ASIC*, vol. 2007, pp. 974–977, 2007.

[19] Y. Guo, F. Yuan, Y. Chang, Y. Kou, and X. Zhang, "A bootstrap structure directly charged by BUS voltage with threshold-based digital control for high-speed buck converter," *Electronics*, vol. 10, no. 22, p. 2863, 2021.

[20] Z. Zhou, X. Ming, B. Zhang, and Z. Li, "Design of Novel Bootstrap Driver Used in High Power BUCK Converter," *IEEE 8th International Conference on ASIC*, vol. 2009, pp. 1165–1168, 2009.

[21] J. Kacetl, T. Kacetl, M. Jaensch, and S. M. Goetz, "Novel low-side/high-side gate drive and supply with minimum footprint, high power density, and low cost for silicon and wide-bandgap transistors," *IEEE Transactions on Power Electronics*, vol. 36, no. 7, pp. 8219–8229, 2021.